

Large-scale Barrier Dynamics Experiment II (BARDEX II): Experimental design, instrumentation, test program, and data set

Gerd Masselink ^{a,*}, Andrea Ruju ^a, Daniel Conley ^a, Ian Turner ^b, Gerben Ruessink ^c, Ana Matias ^d,
Charlie Thompson ^e, Bruno Castelle ^f, Jack Puleo ^g, Veronica Citerone ^g, Guido Wolters ^h

^aSchool of Marine Science and Engineering, University of Plymouth, Plymouth, PL4 8AA, UK

^bSchool of Civil and Environmental Engineering, University of NSW, Sydney, NSW 2052, Australia

^cFaculty of Geosciences, Utrecht University, Utrecht, 3508 TC, the Netherlands

^dCIMA, Universidade do Algarve, Campus de Gambelas, 8005-139 Faro, Portugal

^eOcean and Earth Science, University of Southampton, European Way, Southampton, SO14 3ZH, UK

^fNRS, Université Bordeaux 1, UMR 5805-EPOC Avenue des Facultés, F-33405, Talence, France

^gCenter for Applied Coastal Research, University of DE, Newark, DE, USA

^hDeltares, Rotterdamseweg 185, Delft, 2629 HD Delft, the Netherlands

Abstract

Despite the increased sophistication of numerical models and field techniques for investigating wave-induced nearshore sediment transport and ensuing beach morphological response, there remains a significant demand for large-scale laboratory experiments to address this research topic. Here, we describe the Barrier Dynamics II Experiment (BARDEX II), which involved placing a near prototype-scale sandy barrier in the middle of the Delta Flume in the Netherlands and subjecting the structure to a range of wave, tide, and water level conditions. A unique aspect of the experiment was the presence of a lagoon behind the barrier, as often occurs in natural barrier settings, providing a convenient means to experimentally manipulate the groundwater hydrology within the barrier. The overall aim of the BARDEX II was to collect a large-scale data set of energetic waves acting on a sandy beach/barrier system to improve our quantitative understanding and modeling capability of shallow water sediment transport processes in the inner surf, swash, and overwash zone. In this paper, we introduce BARDEX II and provide a detailed description of the experiment, including the experimental design, instrumentation, test program, and data set, as well as presenting some examples of the morphological and hydrodynamic data set. We also reflect objectively on the strengths and weaknesses of the data set. This paper serves as an introduction to a special issue of Coastal Engineering, solely devoted to the results of BARDEX II

1. Introduction

Numerical models and field techniques for investigating wave-induced nearshore sediment transport and ensuing beach morphological response have become increasingly sophisticated over the years (e.g., Falchetti et al., 2010; Puleo et al., 2013). One could argue that the increased complexity captured by the models and the enhanced field measuring capabilities would make physical laboratory experiments superfluous; however, there remains a significant demand for large-scale laboratory experiments to address this research topic (Sanchez-Arcilla et al., 2011). In the EU, and funded through Hydralab (<http://www.hydralab.eu/>), large-scale wave flume experiments have been regularly conducted in the GWK flume in Hannover, Germany (e.g., Lopez de San Roman-Blanco et al., 2006), the CIEM flume in Barcelona, Spain (e.g., Stratigakia et al., 2011), and the Delta Flume in Vollenhove, the Netherlands (e.g., Williams et al., 2012a). The large-scale experiment described in this paper took place in the Delta Flume and the setting modeled by this experiment is a sandy barrier system backed by a lagoon. Barrier systems are natural means of coastal protection against flooding, while at the same time representing porous boundaries that connect the terrestrial groundwater table with sea level. Two key processes that are of particular relevance to these two functions, and for which our understanding is far from complete, are swash/overtopping/overwash processes during extreme wave and water-level conditions, and cross-barrier groundwater fluxes. Accurate prediction of the occurrence and morphological consequence of overtopping and overwash is of obvious importance for coastal flood risk assessment and management (Matias et al., 2008). Equally apparent is the relevance of being able to quantify and model cross-barrier groundwater fluxes, for example, for assessing the dispersal of pollutants from coastal aquifers into the sea and saline intrusion as a result of sea-level rise (Andersen et al., 2007). A less obvious but potentially significant and related process is the effect of interactions between the beach groundwater table and swash motion on sediment transport processes on the upper beach (Turner and Masselink, 1998) and, therefore, beach stability. These interactions are strongly controlled by the elevation of the beach groundwater table relative to sea level, and it is often considered that a low water table promotes beach stability, while a high water table has a destabilizing effect on the beach.

In 2008, the large-scale Barrier Dynamics Experiment (BARDEX), funded under the Hydralab III program, was carried out in the Delta Flume to investigate swash, overtopping and overwash processes, cross-barrier groundwater fluxes, and the role of the beach groundwater table on beach stability (Williams et al., 2012a). BARDEX involved placing a near prototype-scale gravel barrier (height 4.5 m; width 30 m) in the middle of the flume and subjecting the structure to a range of wave, tide, and water level conditions. A unique aspect of BARDEX was the presence of a lagoon behind the barrier, as commonly occurs in natural barrier settings, providing a convenient means to experimentally manipulate the groundwater hydrology within the barrier. The main results of this experiment have been published in a 6-paper special issue of Coastal Engineering (Masselink and Turner, 2012; Matias et al., 2012; Thompson et al., 2012; Turner and Masselink, 2012; Williams et al., 2012a,b). The main BARDEX partners considered it appropriate and timely to carry out a second experiment in the Delta Flume, but this time on a sandy barrier. Funding was obtained under the Hydralab IV program, and the project, named BARDEX II to acknowledge its pedigree, was carried out from May to July 2012.

The difference in barrier morphology and sedimentology between the gravel barrier during BARDEX and the sandy barrier during BARDEX II is expected to give rise to significant differences in morphological evolution and hydrodynamics. Specifically, the reduced hydraulic conductivity on the sandy barrier is likely to limit the influence of swash infiltration and barrier through-flow. The sandy barrier is also expected to experience erosive conditions and nearshore bar formation, which could not be achieved on the gravel barrier. Sediment transport processes on the gravel barrier were mainly onshore and through bed load; on the sandy barrier both onshore and offshore transport and both bed load and suspended load are expected to be important. Finally, it is anticipated that the threshold between overtopping and overwashing is significantly different between the sandy and gravel test cases.

* Corresponding author.

E-mail address: g.masselink@plymouth.ac.uk (G. Masselink).

The data set collected during BARDEX II is not only relevant in providing direct comparison with the gravel barrier data set (thereby providing added value to BARDEX), but the sandy barrier data are also important in their own right by providing fundamental new information on cross-shore sediment transport processes in the nearshore zone of sandy beaches. Specifically, in addition to explicitly addressing the effect of swash/groundwater interactions to sediment transport and morphological development in the swash zone, the project also investigates the sediment exchange between the swash and surf zone and, related, the dynamics of nearshore bar systems. It is generally accepted that mean offshore-directed flows are responsible for beach erosion and offshore bar migration under energetic wave conditions, but there is considerable debate in the literature as to what causes beach accretion and onshore bar migration under calm wave conditions. There have been a number of processes proposed that may be implicated in onshore sediment transport, berm construction, and bar migration, including (1) onshore mass flux due to cell circulation (Aagaard et al., 2006); (2) sediment stratification (Conley et al., 2008); (3) turbulence associated with breaking waves and bores (Butt et al., 2004); (4) cross-shore velocity skewness ('wave skewness'; Marino-Tapia et al., 2007); (5) cross-shore velocity acceleration skewness ('wave asymmetry'; Hoefel and Elgar, 2003); (6) ventilated boundary layer (Conley and Inman, 1992); and (7) plug flow due to horizontal pressure gradients (Foster et al., 2006). These different processes are not necessarily mutually exclusive and all, except (1), are addressed during BARDEX II.

2. Organization, aim, and objectives

BARDEX II took place over a 3-month period from May to July 2012 in the Delta Flume, the Netherlands. A total of 58 project days were allocated to the project, comprising 30 days for barrier construction and installation of instruments and pumps, 20 experiment days, and 8 days for decommissioning the experiment. The project was funded under Hydralab IV at a total cost of €353 k, and the project was coordinated by Deltares. The academic lead was provided by the University of Plymouth (Gerd Masselink, UoP) and, in addition to the technical staff at the facility, 13 academics, 6 post-docs, 5 PhD students, 4 MSc students, and 6 technicians from 8 institutions and 6 countries participated in the project. The following universities were involved with BARDEX II: Algarve (UAlg), Bordeaux (UB), Delaware (UoD), New Hampshire (UoNH), New South Wales (UNSW), Plymouth (UoP), Southampton (UoS), and Utrecht (UU).

The overall aim of BARDEX II was to collect a near prototype data set of energetic waves acting on a sandy beach/barrier system to improve our quantitative understanding and modeling capability of shallow water sediment transport processes in the inner surf, swash, and overwash zone. The project was structured through 6 work packages (WPs), each with its own set of objectives (the references provided for each of the WPs refer to papers in a 2013 special issue of the *Journal of Coastal Research* and this special issue):

- WP1—barrier hydrology: to observe, quantify, and model the dynamic groundwater conditions within the barrier, subject to varying wave, water-level, and back-barrier lagoon conditions (Lead: Ian Turner, UNSW; Turner et al., 2013; Turner et al., 2016).
- WP2—swash and berm dynamics: to examine the relative roles of nonlocal turbulence advected into the swash zone by turbulent bores versus local turbulence generated in the swash zone by bed shear stress in driving sediment transport processes in the swash zone; to resolve the role of barrier hydrology in controlling equilibrium morphological response at the beachface (Lead: Daniel Conley, UoP; Brinkkemper et al., 2016; Puleo et al., 2016; Ruju et al., 2016; Ruju et al., submitted for publication).
- WP3—swash–surf zone exchange and bar dynamics: to determine and quantify the dominant hydrodynamic and sediment transport mechanisms responsible for swash–surf zone sediment exchange; to identify key processes responsible for onshore and offshore bar migration (Lead: Gerben Ruessink, UU; Winter et al., 2013; Ruessink et al., 2016).
- WP4—barrier overwash: to quantify overwash threshold for different wave and water-level conditions; to investigate the effect of groundwater gradients on overwash processes; to compare overwash processes on sand and gravel barriers (Lead: Ana Matias, UAlg; Matias et al., 2013; Blenkinsopp et al., 2016; Matias et al., 2016).
- WP5—Sediment resuspension and bed morphology: to observe and measure vortex resuspension processes and bedform dynamics under shoaling and breaking waves; to quantify changes in the magnitude and direction of sediment transport (bedload and suspended load) in the region just outside the surf zone (Lead: Charlie Thompson, UoS; Thompson et al., 2013; Kassem et al., submitted for publication).
- WP6—numerical modeling: to further develop and rigorously test advanced process-based cross-shore hydro-morphodynamic models that address bar and barrier dynamics, and barrier destruction through overwash (Lead: Bruno Castelle, UB; Castelle et al., 2013; Dubarbier et al., 2015).

This paper provides a description of the experiment, including the experimental design, instrumentation, test program, and data structure, and provides an introduction to 7 subsequent papers, covering the BARDEX II WPs. An important deliverable of this project is the collection of a comprehensive and state-of-the-art data set on sandy beach

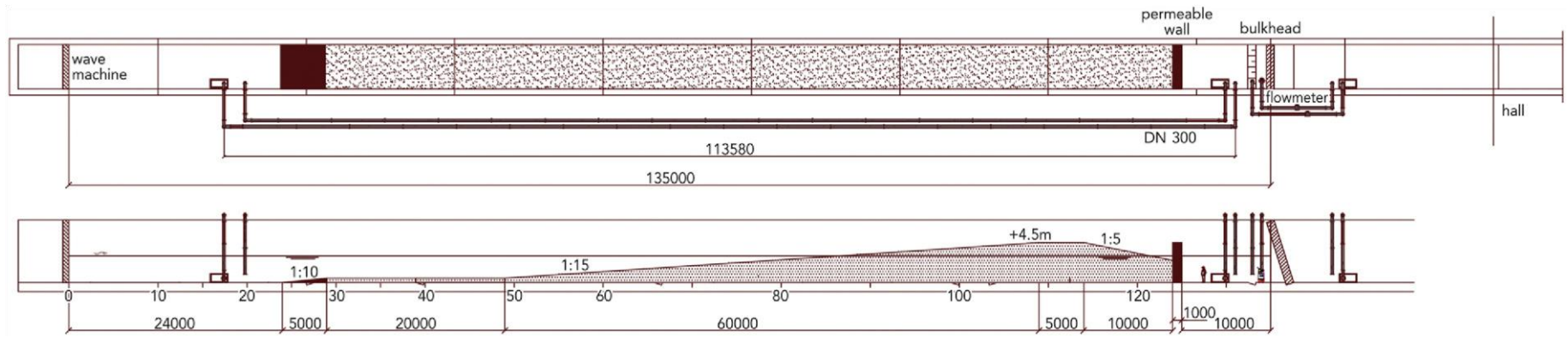


Fig. 1. CAD drawing of experimental set-up in the Delta Flume during the BARDEX II experiment, showing plan view and longitudinal section of the flume. Distances are in mm.

response to changing wave and water level conditions and to ensure that this data set is available to the international coastal research community. Therefore, considerable effort was expended on collating all the data collected as part of BARDEX II in a NetCDF database that contains all the necessary data and metadata to enable data analysis. This paper therefore also serves to 'advertise' and provide context to the BARDEX II data set to facilitate its wider use.

3. Experimental set-up

Fig. 1 shows a CAD drawing of the experimental design during the BARDEX II experiment and includes the along-tank cross-section and the planform view. The origin of the coordinate system is the rest position of the wave paddle at the back of the flume ($x = 0$ m), the center line of the flume ($y = 0$ m), and the flume floor ($z = 0$ m). Positive x is from the paddle to the front of the flume, positive y is toward the left of the positive x -axis, and positive z is upward from the flume floor.

A 4.5-m-high and 75-m-wide sandy barrier was constructed in the Delta Flume with the crest of the barrier located at 1.5 m above the default mean sea level (MSL) of 3 m and a 10-m-wide lagoon situated to the landward. The sand barrier was separated from the lagoon by a permeable wall constructed out of a steel mesh (grid size = 0.05×0.05 m) shrouded on both sides with two layers of 180 micron geotextile cloth (Geolon PE180) to allow water to move freely between back-barrier slope and lagoon but prevent the ingress of sand into the lagoon during overwash tests. Landward of the lagoon, and separated by an impermeable gate, a reservoir was located which was used as a water buffer to help regulate the water level in the lagoon. Water level in the lagoon ranged between 1.75 m and 4.25 m above the flume floor, representing a water volume of $87.5\text{--}212.5$ m³.

A total of 1365 m³ of sand was used to construct the barrier at a cost of just over 10% of the project budget. The sand was introduced into the flume in small batches and compacted regularly (c. 0.5-m layers). The barrier represents a cross-sectional area of 220 m² and considering a flume width of 5 m, the total amount of compacted sand in the flume was 1100 m³. This represents a compaction of 20%.

Fig. 2 shows the relative and cumulative frequency distribution of the grain size of sediment used. The distribution was obtained by averaging the sieve analysis results of 4 separate sediment samples that were each sub-sampled (using a riffle box) from a large subsample that was collated from c. 300 small samples taken at 2-m intervals from the active part of the beach ($x = 80\text{--}110$ m) after each test series. The sediment size distribution is thus considered representative of the spatially and temporally-averaged sediment characteristics of the BARDEX II barrier. The sediment can be classified as a moderately-sorted, coarse-skewed, medium sand with a small amount of gravel (c. 1%). The median and mean sediment size is 0.43 mm and 0.51 mm, respectively, and the sorting and skewness is 0.81ϕ and -0.24ϕ , respectively. All c. 300 sediment samples were analyzed to investigate spatial and temporal changes in the sediment fall velocity during the experiment. Analysis of 30 samples sub-sampled from a bulk sediment sample collated from all sediment samples collected indicate that the BARDEX II sediment has a median sediment fall velocity of 0.046 m s⁻¹ and an associated (graphic) sorting of 0.007 m s⁻¹. The sediment fall velocity is somewhat low compared to the median sediment size; however, these values are correct and may be related to the composition and shape of the sediment due to its non-beach origin. The temporal variability of the sediment fall velocity across the beach profile during the experiment will be discussed in Section 7.

The sediment used in the experiment was selected to provide sufficient hydraulic conductivity K and porosity P for significant horizontal (through-barrier) and vertical (through-bed) groundwater flows ($K = 0.0005\text{--}0.001$ m s⁻¹; $P = 0.37\text{--}0.42$; analysis by Deltares), but not too large a grain size as to inhibit sediment resuspension and nearshore bar formation. It should be mentioned here that the sediment size obtained was significantly finer than originally requested. It was the intention to construct the barrier out of sand with a D_{50} of 0.6–0.8 mm; however, the high cost associated with such sediment (€100 k) was prohibitive.

The barrier was composed of a number of distinct profile sections (Fig. 3: (1) a 1:10 seaward-sloping concrete toe at $x = 24\text{--}29$ m; (2) a 20-m-wide horizontal section with a 0.5-m-thick sand layer at $x = 29\text{--}49$ m; (3) a 60-m-wide, 1:15 seaward-sloping section at $x = 49\text{--}109$ m; (4) a 5-m-wide crest at $x = 109\text{--}114$ m; and (5) a 10-m-wide, 1:5 landward-sloping section at $x = 114\text{--}124$ m. A 5-m-high retaining wall was used to separate the back-barrier slope from a 10-m-wide lagoon at $x = 125\text{--}135$ m. The lagoon was separated from a large water reservoir that extended from $x = 135$ m to the end of the Delta Flume at $x = 240$ m by an impermeable gate.

To regulate the water levels in the Delta Flume, four pumps were used (Fig. 1): (1) sea to lagoon, (2) lagoon to sea, (3) reservoir to lagoon, and (4) lagoon to reservoir. A computer program was used to control the discharge of the pumps, based on the difference between actual and desired water levels in the sea and lagoon. Each pump had a maximum capacity of 50 l s⁻¹ and the discharge of the pumps between sea and lagoon was recorded to enable quantification of across-barrier water fluxes. Unfortunately, the gate between the lagoon and reservoir leaked by a significant but poorly constrained quantity, and this made an accurate assessment of the across-barrier fluxes difficult.

4. Instrumentation and data acquisition

A suite of instruments and sampling devices were deployed during the experiment. An overview of the position of the instruments provided by the Delta Flume facility and the project partners is provided in Figs. 3 and 4, respectively. A photo record of the experiment is given

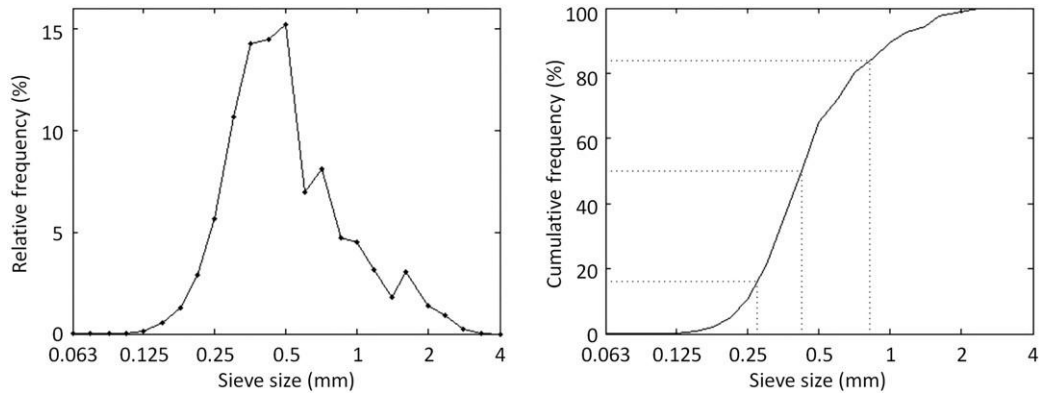


Fig. 2. Relative (left panel) and cumulative (right panel) frequency distribution of grain size of the sediment used in the BARDEX II experiment. The horizontal and vertical dashed lines in the right panel indicate the D_{16} , D_{50} , and D_{84} sediment size, which are 0.28, 0.43, and 0.83 mm, respectively.

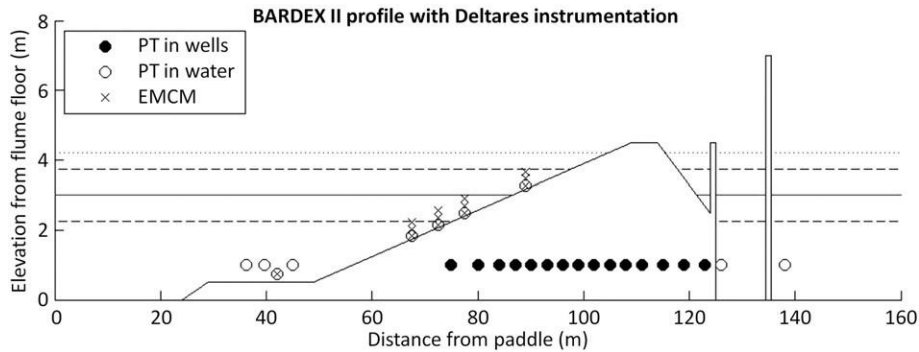


Fig. 3. Delta Flume cross-section with barrier profile at the start of the experiment and location of Deltares instrumentation. PT = pressure transducer; EMCM = electromagnetic current meter. Horizontal solid line shows the 'default' water level used ($h = 3$ m); horizontal dashed lines show the high and low tide 'sea' level and the high and low 'lagoon' level ($h = 2.25$ and 3.75 m). The horizontal dotted line represents the maximum sea level used for the overwash test series D ($h = 4.2$ m). Four separate water bodies or reservoirs can be distinguished: the area between the wave paddle at $x = 0$ and the barrier is referred to as the 'sea'; the small region between the barrier crest and the retaining wall at $x = 124$ m is the 'back-barrier'; the reservoir from $x = 125$ to 135 m is the 'lagoon'; and the reservoir from $x = 135$ m to the end of the flume at 240 m (not shown) is the 'buffer'.

in Fig. 5, while Fig. 6 shows the very densely instrumented section of the scaffold rig for measuring swash dynamics.

The instrumentation provided by the Delta Flume included 28 buried and unburied pressure transducers (PTs) for recording water levels in the sea, lagoon, reservoir and within the barrier itself (groundwater levels); 10 wall-mounted electromagnetic current meters (EMCMs); 3 optical backscatter sensors (OBSs) for measuring suspended sediment concentrations; 3 ARGUS-style video cameras to monitor overwash, swash, and breaking waves; 4 discharge recorders for the pumps and a high-resolution mechanical bed profiler mounted off the carriage to record morphological change. All these data were collected at 20 Hz by the central Delta Flume computer. Beach profiles along the centerline of the flume ($y = 0$ m) were recorded nominally every 30 min (more frequent at the start of the simulations) and a total of 135 profiles were surveyed.

To complement the Delta Flume equipment, a large number of additional instruments were deployed by the project partners (refer to Table 2 for list of acronyms relating to participating institutions and instrumentation used during the experiment):

- Within the barrier—Electric conductivity probes and thermistors were deployed in the sand to measure through-barrier movement of both an environmentally inert groundwater tracer and of heat. In addition, 4 pairs of high-precision PTs, deployed in piezometer tubes, were used to resolve instantaneous groundwater fluxes at the beachface. Data from these instruments contributed mainly to WP1 and were installed and maintained by UNSW (see Turner et al., 2016).
- Swash zone and barrier crest—Equipment for recording swash and overwash flows, suspended sediment fluxes and bed-level changes

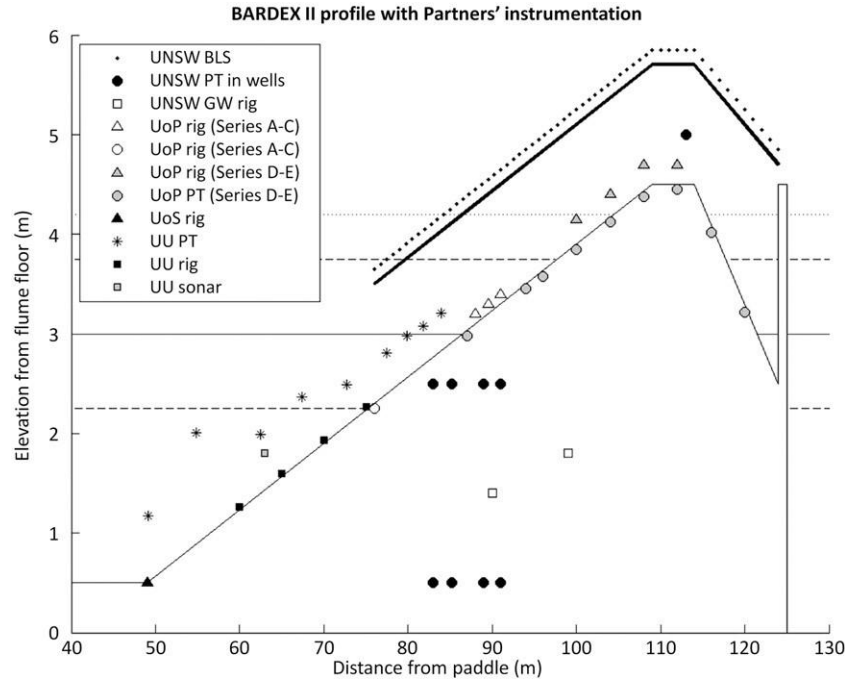


Fig. 4. Close-up of the barrier showing the locations of the instruments provided to BARDEX II by the Project Partners: UNSW = University of New South Wales; UoP = University of Plymouth; UoS = University of Southampton; and UU = Utrecht University. Horizontal solid line shows the 'default' water level used ($h = 3$ m); horizontal dashed lines show the high and low tide 'sea' level and the high and low 'lagoon' level ($h = 2.25$ and 3.75 m). The horizontal dotted line represents the maximum sea level used for the overwash test series D ($h = 4.2$ m). BLS = bed-level sensor; PT = pressure transducer; and GW rig = buried instrument rig with electric conductivity probes and thermistors to measure through-barrier groundwater flows (refer to Turner et al., 2016).

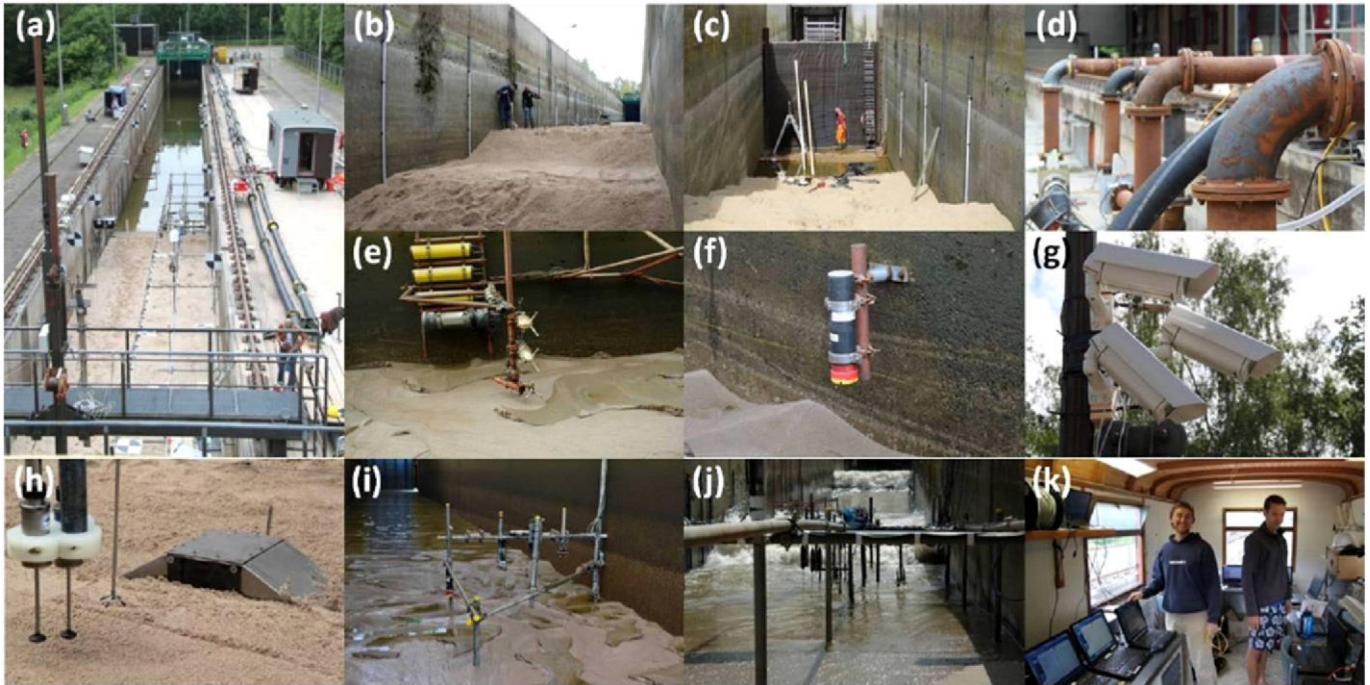


Fig. 5. Photos showing key elements of the experimental set-up during BARDEX II. (a) Overview of the Delta Flume looking from trolley above crest of the barrier toward the wave paddle, 120 m distant. (b) Barrier under construction showing several groundwater wells affixed to the flume wall. (c) Construction of retaining wall separating the back of the barrier from the lagoon. (d) Pump system showing all inlets/outlets to/from the lagoon. (e) Surf zone turbulence rig. (f) Self-logging pressure sensor for measuring surf zone water levels. (g) An Argus video system, comprising 3 cameras, was mounted at a height of c. 5 m above the barrier crest. (h) Underwater video camera flush mounted with the bed collocated with electromagnetic and acoustic current meters for making detailed measurements of hydro- and sediment-dynamics in the boundary layer (only during test A5). (i) Offshore rig with a range of acoustic instruments to monitor sediment resuspension and bedform dynamics. (j) Photo taken through the scaffold rig showing numerous vertically-mounted electromagnetic and acoustic current meters. (k) View inside one of the measurement cabins with more than 15 laptops that were used simultaneously during the experiment to record the data.

were deployed from a large scaffold rig comprising 6 EMCMS, 6 acoustic Doppler velocimeters (ADV) for point measurements, 4 acoustic Doppler velocity profilers referred to as Vectrinos (VECs), 6 OBSs, 8 PTs, 45 acoustic bed-level sensors (BLSs; Turner et al., 2008), and 6 conductivity concentration profilers (CCPs; Lanckriet

et al., 2013). In addition, a thermal camera and 2 LiDARs were used to remotely monitor swash motion. These instruments were looked after by UoP, UoD, UNSW, and UoNH; their data contributed mainly to WP2 and WP4 (see Ruju et al., 2016).

- Surf zone – Equipment for measuring surf zone flows, breaking waves, turbulence, and suspended sediment concentrations were deployed from 3 wall-mounted rigs, each comprising 1 EMC, 1 PT, and 3 OBSs, and one rig comprising 3 ADVs, 1 PT, and 7 OBSs. In addition, a 3D sector scanning sonar (SONAR) was deployed to monitor bedforms in the surf zone and a cross-shore array of 9 self-logging PT were deployed across the entire seaward slope of the barrier to record water levels and wave propagation. UU was responsible for the surf zone instrumentation and the data contributed mainly to WP3 (see Brinkkemper et al., 2016).
- Shoaling wave zone—A single measurement rig was deployed just beyond the zone of breaking waves to measure hydrodynamics, sediment resuspension, and bedforms under shoaling waves. The rig comprised solely of acoustic devices and included 2 ADVs, 2 sand ripple profilers (SRPs), an acoustic backscatter sensor (ABS), and a SONAR. The data contributed mainly to WP5 and were collected by UoS.

Data collected with these additional instruments were logged at frequencies ranging from 4 to 64 Hz using a suite of laptops and data loggers.

All data were recorded in GMT. The data collected by the project partners were recorded on a bank of laptop computers all timesynced using GPS clock and a local network (one of the laptops operated as a time server). Except on 14 and 15 June 2012, the time server worked throughout the experiment and the data collected by the partners are therefore on the same time. Unfortunately, the time synchronizing with the Delta Flume computer did not work and these instruments are on their own time. To time-synch both data sets on an ad hoc basis, co-located instruments (e.g., some BLSs were located at very similar x-coordinates to the Delta Flume PTs) can be used. The video data were time-synched with the other data collected by the Delta Flume computer using a strobe light that was triggered at the start of the image collection. This trigger signal was also logged as a voltage with the other Delta Flume instruments allowing synchronizing the video images with the hydrodynamic data.

5. Experimental procedure

5.1. Test program

The test program consists of 19 distinct ‘tests’ with different wave and water level conditions making up 5 ‘test series’ (Table 1). • Test series A—The objective of this test series was to determine the effect of high and low lagoon level, and therefore high and low beach groundwater table, on swash sediment transport processes and beach profile development. Two different wave conditions (accretion and erosion) and three different lagoon levels (low, medium, and high) were used.

- Test series B—During this test series, the effect of lowering the sea level on nearshore bar development was addressed. Erosive wave conditions were used and the sea level was lowered by 0.5 m relative to the default sea level.
- Test series C—To investigate tidal effects on beach profile development, the beach was subjected to a low–high–low tide cycle with erosive wave conditions. The tidal cycle, which had a range of 1.5 m and a



Fig. 6. Schematic and photo of the main swash instrumentation on the scaffold rig at $x = 89.5$ m. Instrumentation includes, from left to right, 1 bed-level sensor (BLS), 2 acoustic Doppler current meter profilers (Vectrino II), 2 partly buried conductivity concentration probes (CCPs), 2 pairs of mini electromagnetic current meters (EMCMs), 2 buried pressure transducers (PTs), 1 bed camera (BC), 2 optical backscatter sensors (OBSs), 1 acoustic Doppler current meter for point measurements (Vectrino I). There are three instruments in the photograph that are not present on the schematic: a Vectrino II in the far left of the photo is offset by 1.5 m 'landward' of the main swash rig (at $x = 91$ m); another Vectrino II is located between the Vectrino II and the central scaffold pole, and is offset by 1.5 m 'seaward' of the main swash rig (at $x = 88$ m); and the feature attached to a scaffold pole in the far right of the photo is a self-logging PT offset by 5.6 m 'seaward' of the main swash rig (at $x = 83.9$ m).

period of 12 hours, was segmented in 30-min tide steps (refer to Section 5.3). To enhance the effect of the beach groundwater table generally lagging behind the tidal water level, the rising tide was executed with a low lagoon level and the falling tide with a high lagoon level. The computer-controlled pump system was used to keep the lagoon levels constant by pumping water out of the lagoon into the sea during the rising tide and from the sea into the lagoon during the falling tide.

- Test series D—During this test series, the water level was incrementally raised by 0.15-m intervals for 7 different wave conditions (constant height, but variable period) to achieve a sequence of swash–overtopping–overwash. For each test condition, 20 min of wave action was used.
- Test series E—During this final test series of the experiment, the sea level was set just beyond the overwash threshold and the barrier was exposed to consecutive 13-min segments of energetic overwash conditions. These conditions resulted in progressive lowering of the bar crest and sediment transport across the barrier crest into the back-barrier region. Fig. 7 shows a sequence of photos taken during overwash conditions (see Matias et al., 2016).

Fig. 8 shows the wave and water level conditions encountered during all tests. The different test series were sequenced such that they represent an increased level of complexity. Test series E continued until the barrier was lowered so much that unidirectional flow occurred across the barrier crest into the lagoon because the lagoon-to-sea pump could not keep up with the overwashing.

The beach-barrier morphology was not reshaped between the different test series because, as well as requiring valuable test time, this was impossible without removing most of the instrumentation. Reshaping of the back of the barrier did take place after each of the tests during test series D because during overwash, a distinct channel developed in the center of the flume. This channel was manually filled in to avoid affecting the flow conditions during the next test condition. During test A7, a channel developed in the swash zone, possibly related to the high-lagoon level enhancing groundwater outflow, and the swash was distinctly three-dimensional. It was attempted to straighten this morphology using a short period of regular wave forcing (only partly successful). The swash flow pattern during tests with erosive wave conditions was overwhelmingly two-dimensional, but the accretionary test conditions (tests A6–A8) had a significant three-dimensional swash flow component.

5.2. Wave steering

For irregular waves, the wave paddle steering signal was a JONSWAP spectrum specified using significant wave height H_s and peak wave period T_p with a peak-enhancement factor γ of 3.3. The exact wave steering signal required to produce a certain wave spectrum depends on the water depth in front of the wave paddle, and the gain needs adjusting when the same wave signal needs to be reproduced for varying water depths. The Automated Reflection Compensator (ARC) was deployed at all times to avoid seiching in the flume. To enable comparison between different tests within the same test series, for tests with

Table 1
Overview of the planned experimental program during BARDEX II. H_s = significant wave height; T_p = peak wave period; h_s = sea level; h_l = lagoon level; and T_{test} is duration of the test. Note that these planned conditions are not identical to the conditions that actually took place (refer to Fig. 8). Where double values or a range of values are indicated for the parameters, the forcing conditions were varied during the test.

Test	H_s (m)	T_p (s)	h_s (m)	h_l (m)	T_{test} (min)
Test series A: Beach response to varying wave conditions and different lagoon levels; no tide					
A1	0.8	8	3	3–3.4	320
A2	0.8	8	3	4.3	200
A3	0.8	8	3	4.3	180
A4	0.8	8	3	1.75	200
A5	0.3–0.8	8–12	3	1.75	17
A6	0.6	12	3	3	335
A7	0.6	12	3	4.25	213
A8	0.6	12	3	1.75	200
Test series B: Bar dynamics due to different sea levels; no tide					
B1	0.8	8	3	1.75	165
B2	0.8	8	2.5	1.75	255
Test series C: Beach response to varying wave conditions with tide (30-min data segments)					
C1	0.8, 0.6	8	2.25 → 3.65	1.75	330
C2	0.8, 0.6	8	3.53 → 2.25	4.25	270
Test series D: Identification of overtopping/overwash threshold; increase sea level until overwash occurs (20-min data segments)					
D1	0.8	4	3.15 → 4.2	1.75	160
D2	0.8	5	3.45 → 4.05	1.75	100
D3	0.8	6	3.45 → 3.9	1.75	80
D4	0.8	7	3.45 → 3.9	1.75	80
D5	0.8	8	3.45 → 3.75	1.75	60
D6	0.8	9	3.30 → 3.75	1.75	80
D7	0.8	10	3.15 → 3.6	1.75	80
Test series E: Barrier overwash (13-min data segments)					
E	0.8	8	3.9	1.75	65

the same wave forcing (H_s and T_p), the identical wave steering signal was used. The wave steering signals were segmented into separate ‘runs’ to allow frequent interruption of the wave forcing for beach profile measurement, and also for instrument maintenance to ensure that near-bed measurements were being made.

Accretionary and erosive wave conditions were used. It was the intention to start with accretionary wave conditions ($H_s = 0.8$ m; $T_p = 8$ s), followed by erosive wave conditions ($H_s = 1$ m; $T_p = 4$ s). However, due to the sediment size being significantly finer than planned, the ‘accretionary’ wave condition (tests A1–A4) resulted in beach erosion; therefore, the second wave condition, which was supposedly erosive (tests A6–A8), was modified ($H_s = 0.6$ m; $T_p = 12$ s). Example spectra and time series of the two wave conditions are shown in Fig. 9. The deep water wave steepness values H/L for the accretionary and erosive conditions are 0.003 and 0.008, respectively. Assuming a sediment fall velocity of 0.046 m s⁻¹, the accretionary and erosive wave conditions represent dimensionless fall velocities $\Omega = H_s/w_s T_p$ of 1.1 and 2.2, respectively.

During test series A, a several-hour-long erosive and accretionary wave steering signal was made for a water depth of $h = 3$ m. During

Table 2
Overview of the key acronyms relating to participating institutions and instrumentation used during the experiment.

Institutions	Instrumentation
UAlg = University of Algarve	ABS = acoustic backscatter sensor
UB = University of Bordeaux	ADV = acoustic Doppler velocimeters
UNSW = University of New South Wales	BLS = acoustic bed-level sensor
UoD = University of Delaware	CCP = conductivity concentration probe
UoNH = University of New Hampshire	EMCM = electromagnetic current meters
UoP = University of Plymouth	OBS = optical backscatter sensors
UoS = University of Southampton	PT = pressure transducer
UU = University of Utrecht	SONAR = 3D sector scanning sonar
	VEC = Vectrino

the tests, this long wave steering signal was divided in periods of variable length to allow for beach profiling and instrument adjustment between the periods of wave forcing. During most tests of test series A, irregular wave action was followed by 5 min of mono-chromatic waves and 15 min of bi-chromatic waves. Except for the first mono and bi-chromatic tests, which were too energetic, the mono- and bichromatic wave heights were selected to ensure that the wave energy associated with these signals was the same as that for the random wave signal. The mono-chromatic runs were carried out to enable the derivation of an ensemble-wave signal for detailed study of boundary layer dynamics and the bi-chromatic runs were designed to provide insights into the effects of wave groups of sediment resuspension and beachface adjustment. Test A5, conducted between erosive tests A3 and A4, involved 8 short sequences of mono- and bi-chromatic wave action (2 min each) and was specifically designed to make controlled and detailed measurements of boundary layer processes (refer to Fig. 5h).

For test series B, the erosive wave signal was used, but wave steering was adjusted for reduced water depth during test B2. During test series C, the sea level was varied to simulate a tidal cycle (refer to Section 5.3). The 12-hour tidal signal was subdivided into 25×30 -min segments with constant water depth during the segments. For each segment, the erosive wave steering signal was used, but adjusted for water depth. So, an identical sequence of waves occurred during each segment.

During test series D, each segment had 20 min of wave action and water depth was increased in 0.15-m intervals until overwashing occurred. The wave sequence was identical for each run, but the wave steering signal was adjusted for changing water depth and wave period. During test series E, the barrier was subjected to overwash conditions with a constant water level and wave forcing. The erosive wave steering signal was used during test series E, but only in 13-min segments.

5.3. Tidal signal

During test series C, a tidal cycle was simulated. The tidal signal was a ‘proper’ sinusoid with an amplitude of 0.75 m and a period of 12 hours, but the signal was ‘cut’ into 30-min segments, each with a constant water depth (Fig. 10). This was required because otherwise the ARC cannot be engaged with a slowly changing water level, and this would have resulted in significant seiche in the tank (this problem occurred during BARDEX). The maximum difference in water level between two consecutive 30-min segments was 0.2 m. The JONSWAP wave steering signal for each segment was identical, although adjusted for water depth, to ensure that any recorded morphological changes were not due to changing wave conditions. It was observed that as high tide was approached, overtopping started to occur; therefore, H_s was decreased from 0.8 m to 0.6 m, and the four planned segments at and around high tide were not executed. Some wave breaking off the paddle occurred during the lower water levels (also during test B2).

5.4. Maintenance of instrument elevations

Positional control of the instrumentation was critical, especially when measurements are aimed at collecting near-bed data (refer to Fig. 6). The instruments that remained fixed in position throughout the experiment include all Delta Flume instrumentation (PTs in the groundwater wells and wall-mounted EMCMs, PTs, and OBSs), the self-logging PTs across the surf zone, and the instruments on the offshore rig (VECs, ABS, SRPs and SONAR). The BLSs also remained in position, but between test series C and D, the lower 15 BLSs were moved from the seaward side of the scaffold rig to the lagoon side (refer to Fig. 4). Regular total station surveys were also carried out to ensure that the scaffold rig did not settle over the course of the experiment.

The surf zone rigs were fixed to the flume wall and their x and y coordinates remained constant; however, between runs, the rigs were winched up and lowered to make sure that the elevation of the instruments (ADV, EMCM, PT, and OBS) above the bed was the same at the start of each run. The swash and overwash instruments (VECs, ADVs and EMCMS and OBSs, buried PTs) were deployed to record near-bed hydro- and sediment-dynamics and within-bed pressure gradients,

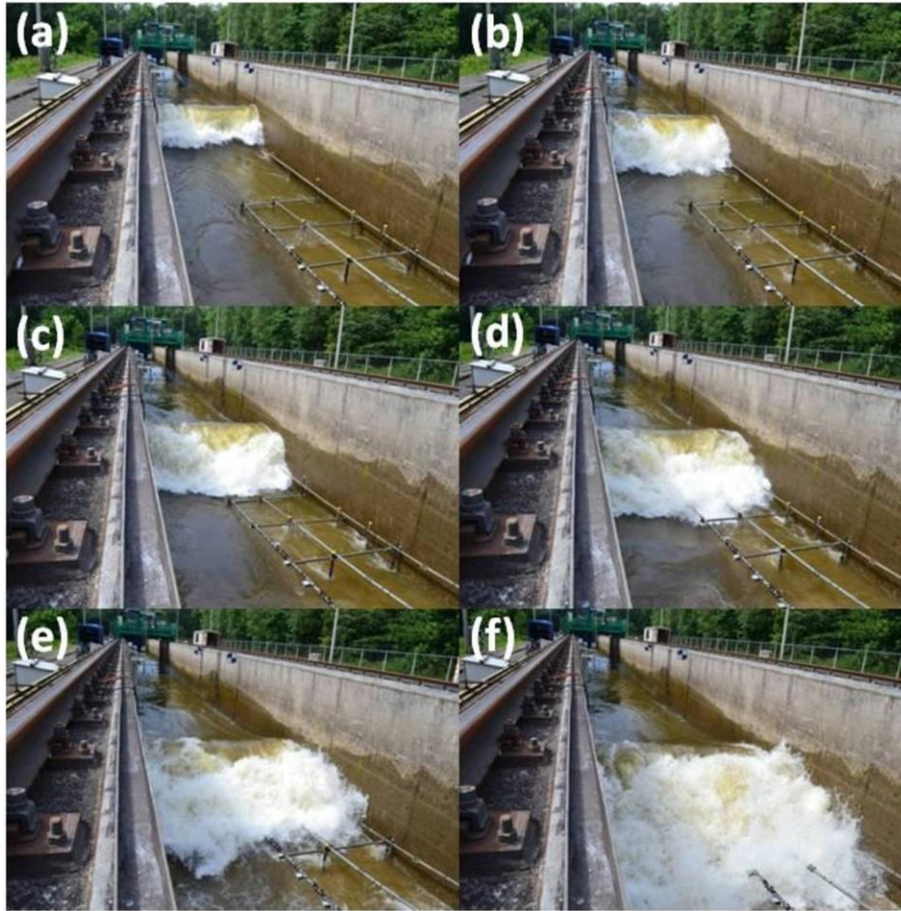


Fig. 7. Photo sequence showing turbulent bore going through the scaffold rig during overwash test series E.

and required frequent manual adjustments (mainly in the vertical, but also in the horizontal). These adjustments were carefully noted and are included in the NetCDF files as metadata (refer to Section 6).

6. Organization of data files

The instrumentation deployed along the wave flume facility measured a range of hydrodynamic and morphodynamic parameters. These devices were logged to different PC platforms and data were collected using separate software packages usually distributed by the instrumentation companies who manufacture the individual sensors. As a result, a heterogeneous data set made up of different format files was collected.

In order to provide an accessible and easy-to-use data set to a wide user-community, the experimental raw data were homogenized and converted into a unique data format. The NetCDF (Network Common Data Form) standard was chosen for this purpose. The main reasons behind this choice was that NetCDF is a self-explanatory and platform-independent format which has been widespread adopted by a large community of geophysical scientists such as climatologists, meteorologists, and oceanographers. Moreover, NetCDF is an open standard ensuring that its specifications are available and can be implemented without the need to pay royalties or license fees.

BARDEX II data are stored in NetCDF files organized in several groups mainly reflecting the collecting systems used during the experiments. Table 3 describes the data set structure. These data include extensive metadata and, accompanied by the associated documentation, are self-explanatory. Positions of the instrumentation including the x, y, and z coordinates in the adopted reference system are included in the metadata. Moreover, it is worth noting that the time series in the original raw data have been split up into shorter time segments, each one containing data from a particular data segment, thus making ease of identifying and working with data from the individual segments. Although NetCDF is a widely adopted data format, potential users of the data are most likely to use Matlab for the data analysis. Therefore, the BARDEX II data set includes Matlab scripts to read in the NetCDF files and convert the data into data structures. The complete data set is freely available from www.hydralab.info.

7. Morphological and sedimentological development

Fig. 11 provides a summary of the morphological development during BARDEX II and indicates 5 main morphological responses (see also Ruessink et al., 2016):

- Bar formation—Erosive conditions prevailed during tests A1–A4. After c. 16 hours of erosive wave action, a small berm developed above MSL at $x = 90\text{--}100$ m (berm volume $Q_{\text{berm}} = 0.5 \text{ m}^3 \text{ m}^{-1}$), but the prevailing morphological development was the formation of a nearshore bar around $x = 70$ m. The bar formed mainly as a result of offshore sediment transport in the lower swash and surf zone and remained the focus of wave breaking throughout these tests.
- Berm formation—Accretionary conditions during tests A6–A8 caused onshore sediment transport, resulting in the disappearance of the pre-existing nearshore bar and the formation of a very pronounced berm at $x = 90\text{--}105$ m. After 11 hours of accretionary wave action, the height of the berm above the original profile was c. 1 m, the

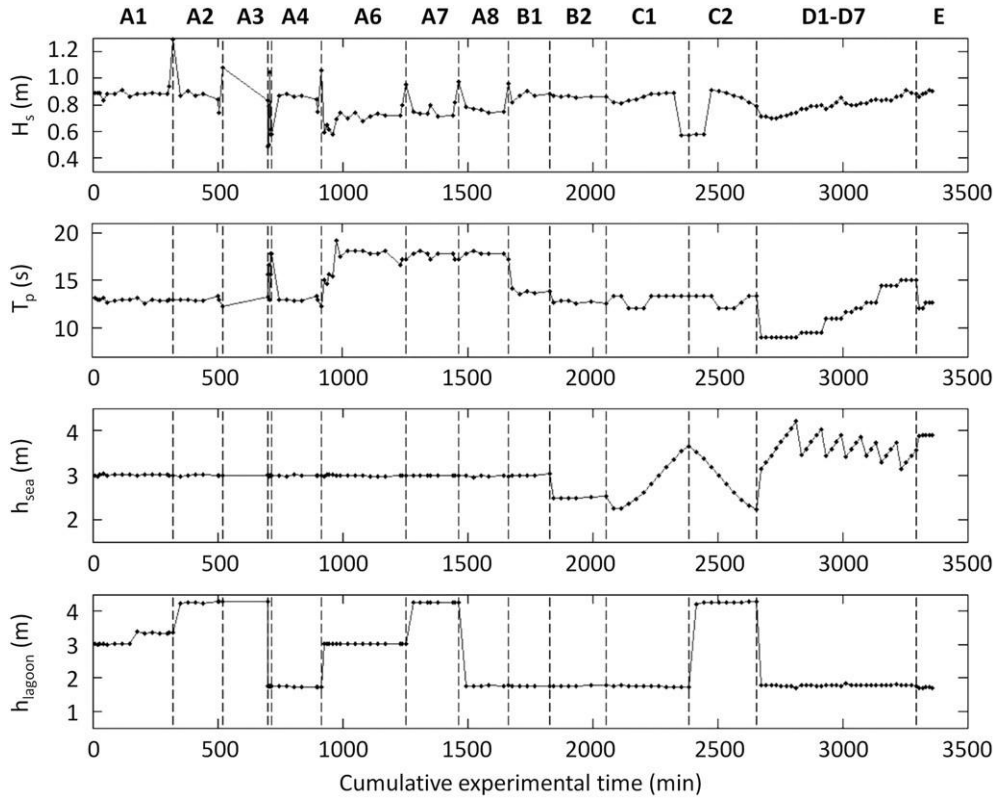


Fig. 8. Measured significant wave height H_s , peak wave period T_p , mean sea level h_{sea} and mean lagoon level h_{lagoon} for all BARDEX II tests. The measured wave conditions were based on the first 512 data points of every test (c. 8 min) of the PT sensor deployed at $x = 36.2$ m (offshore). The pressure data were corrected for depth attenuation using linear theory and a frequency cut-off based on the peak frequency and the water depth, but the signal was not separated into the incoming and outgoing signal. Significant wave height was simply determined as four times the standard deviation of the time series. The mean sea level and the lagoon level were computed over the complete test using the mean of the PT sensor deployed at $x = 36.2$ m and 140 m, respectively. Test A5, which involved 8 short sequences of mono- and bi-chromatic wave action (2 min each) was conducted between tests A3 and A4.

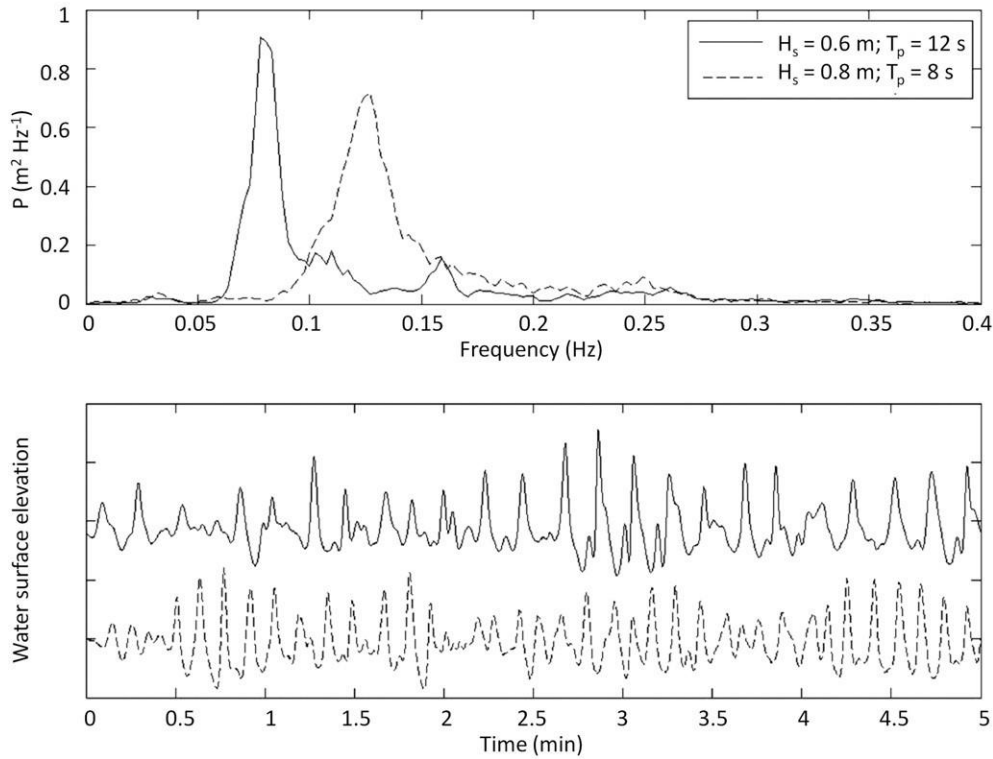


Fig. 9. Example wave spectra (upper panel) and 5-min time series (lower panel) of accretionary ($H_s = 0.6$ m; $T_p = 12$ s) and erosive ($H_s = 0.8$ m; $T_p = 8$ s) wave conditions. The data presented are (vented) pressure data recorded at $x = 42$ m (offshore) and the data are not corrected for depth attenuation. In the lower panel, the time series are offset by 1 m for ease of comparison and the tick marks on the y-axis are at 0.5-m intervals.

beachface gradient had increased from 1:15 to 1:6 and Q_{berm} was $7 \text{ m}^3 \text{ m}^{-1}$.

- Profile stability—During test series B and C, when erosive waves were used and the sea level varied between 2.25 and 3.65 m, the beach profile was relatively stable. Hardly any change occurred in the subtidal area; test series B was of insufficient duration (6 hours) to re-establish a nearshore bar and the lack of a consistent breakpoint position during the tidal test series C also precluded development of bar morphology. The pre-existing berm did undergo some further development, especially at the end of the rising tide when wave runup overtopped the barrier crest and induced vertical accretion. The sediment for this berm accretion was sourced from the lower beachface, where erosion prevailed.
- Overtopping followed by overwash—Almost 12 hours of wave conditions around the overtopping/overwash threshold were simulated during test series D. Over this period, a subdued nearshore bar developed at $x = 80\text{--}85$ m, but, more importantly, the shoreline retreated by c. 6 m and a large amount of sediment was transferred from the beachface to the back of the barrier by overtopping and overwash processes. By the end of each of the overtopping/overwashing test, the barrier was fully saturated as a result of the overwash processes. However, before starting the next test, the barrier was allowed to drain overnight to avoid the saturated conditions affecting the morphological development during the next test. Test D1, with the shortest wave period ($T_p = 4$ s), was anomalous: as the sea level was progressively raised from 3.15 to 4.2 m, rather than transitioning from swash to overtopping to overwash, the beach developed a scarp and a subaqueous bar, while progressively retreating. The developing bar enhanced surf zone dissipation, and despite the increase in the sea level during

Table 3

Overview of the NetCDF data groups with the included instrumentation and measured parameters (data freely available from www.hydrallab.info).

Data Group	Instrumentation	Measured parameters
BLS (290 MB)	BLS	Water and bed levels in the inner surf and swash zone
DELTARES (5.69 GB)	PT, EMCM, OBS Wavemaker Pump Video strobe	Hydrodynamic and morphodynamic quantities along the wave flume (sea and lagoon)
PROFILES (12.9 MB)	Bed profiler	Subaerial and subaqueous beach profile
SOUTHAMPTON (9.35 GB)	ABS ADV SRP	Hydrodynamics, sediment resuspension, and bedforms in the near-bed region extending offshore from the surf zone
SWASH (635 GB)	PT, EMCM, OBS ADV VEC	Velocities, turbulence, water levels, and suspended sediment concentrations in the swash zone
UTRECHT (433 MB)	PT, EMCM, OBS ADV	Mean flows, wave velocities, turbulence, and sediment concentrations in the surf zone

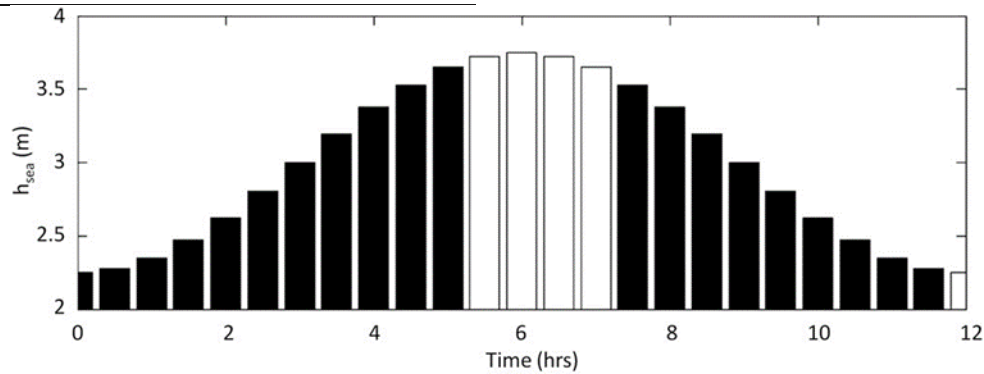


Fig. 10. Tidal signal used during test series C. Because overtopping of the barrier crest started to occur close to high tide, only the water levels presented by the black bars were carried out.

D1, the runup elevation remained more or less constant for a long time, suppressing the overtopping of the barrier and the transition to overwash. During the other D tests, the beach prograded and demonstrated net accretion of the berm crest, while also showing transfer of material to the back of the barrier and into the lagoon.

- Persistent overwash—During test series E, the overwash condition for $T_p = 8$ s was maintained for just over an hour (5 runs of 13 min each). Continuous and energetic barrier overwash occurred under these conditions (refer to Fig. 7) and resulted in c. 3 m shoreline retreat, lowering of the barrier crest and the transfer of $6 \text{ m}^3 \text{ m}^{-1}$ of sediment from the crest of the barrier to the back-barrier region. Similar to observations during the first BARDEX (Matias et al., 2012), barrier crest lowering was enhanced by positive feedback through the positive link between the reduction in barrier freeboard and the increase in overwash frequency.

As a measure of the rate of morphological response, Fig. 12 plots the change in sediment volume of the upper beach ('berm') region of the beach ($x = 90\text{--}110$ m) Q_{berm} relative to the volume at the start of the experiment, and the gross rate of volumetric change over this region Q_{berm}/dt for each run. Values for Q_{berm}/dt range from 0 to $0.1 \text{ m}^3 \text{ m}^{-1} \text{ min}^{-1}$ and are highest during the overwash test series. The accretionary conditions (tests A6–A8) are characterized by larger Q_{berm}/dt values than the erosive wave conditions (tests A1–A4; test series B and C), and the small spikes in the Q_{berm}/dt time series are related to mono- and bi-chromatic wave action. From a relaxation and morphological equilibrium point of view, it is interesting to note that there is practically a linear build-up of the berm over the 12-hour period ($t = 900\text{--}1700$ min) during the accretionary wave conditions of test series A.

After each test, the active part of the beach profile (from $x = 80$ to 110 m) was sampled at 2-m intervals and the sediment fall velocity was determined for all the samples. The mean sediment fall velocity of the barrier sediment, computed by taking into account all sediment samples, was 0.046 m s^{-1} ; however, the fall velocities varied considerably in time and space (Fig. 13). The fall velocity was very uniformly distributed across the beach at the start of the BARDEX II experiment (see 'pre' in Fig. 13), but during test series A, the barrier crest region became finer ($w_s = 0.03\text{--}0.04 \text{ m s}^{-1}$) and the mid-lower swash zone and inner surf zone became significantly coarser ($w_s = 0.06\text{--}0.08 \text{ m s}^{-1}$). After test B2 (0.5-m lower sea level) and test series C (rising and falling tide), the cross-shore sediment distribution became much more uniform and no further changes occurred during the overtopping and overwash runs of test series D and E.

8. Example of hydrodynamic data

Fig. 14 shows a 6-min example time series of hydrodynamics measured along the wave flume for run no. 2 of test A2 (swash; A2_02). In the first and second panels, the evolution of the free surface elevation estimated from 2 PT signals at separate cross-shore locations is plotted. The third panel displays the water

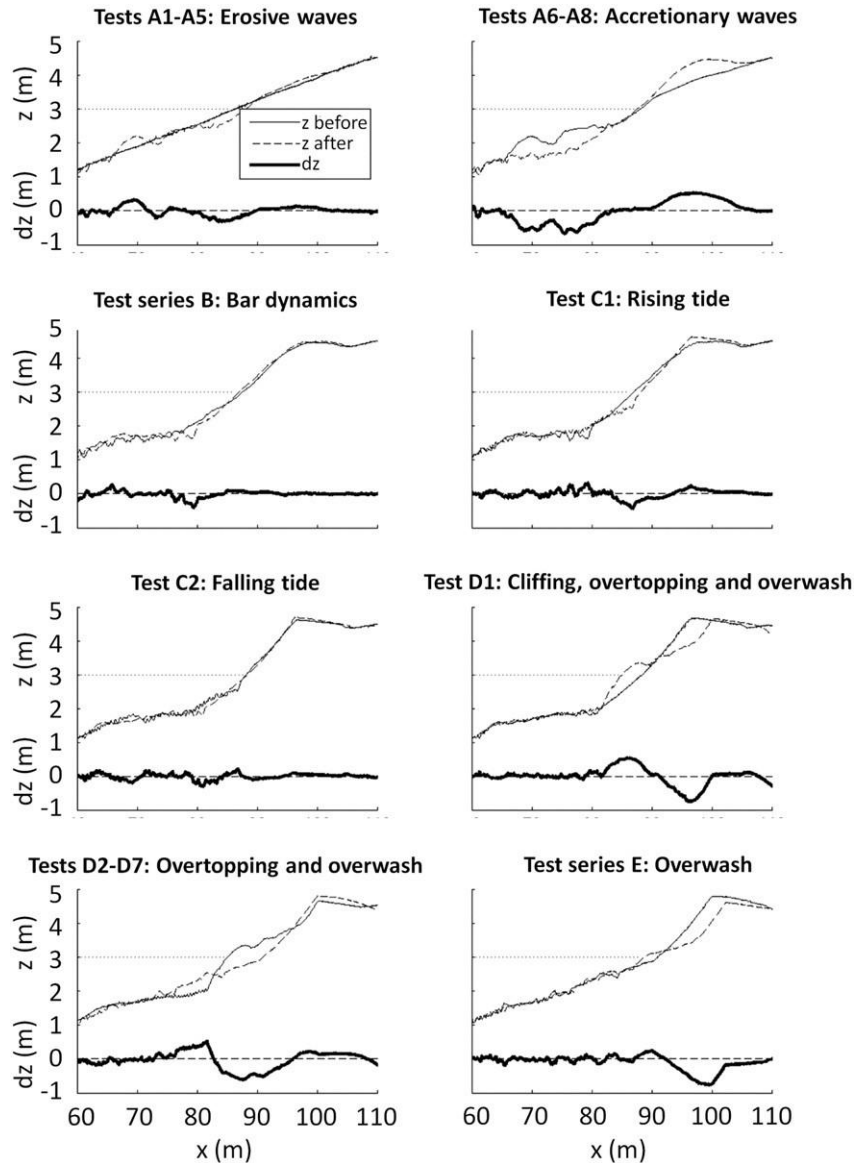


Fig. 11. Beach profiles and morphological change for distinct periods of the test program.

elevations as well as the bed level detected by a swash BLS. In these upper three panels, an individual wave event found approximately in the middle of the time series is marked by a down-facing triangle in order to spotlight the propagation along the flume. The fourth and the lower panels show the groundwater level fluctuations measured by a buried PT and the time stack of swash motions on the beach face. Fig. 14 highlights the propagation of waves as groups evolve approaching the shoreline, eventually forcing runup oscillations and groundwater fluctuations on the beach face and in the barrier. The concept of the beach acting as a low-pass filter is also clearly illustrated. The BLS time series (third panel for $x = 90.2$ m) shows that the swash processes during the 6-min segment resulted in bed accretion.

9. Lessons learned and main conclusions

This concluding section provides a summary of the main methodological lessons learned and the key findings of the project as reported in the papers of this special issue of Coastal Engineering.

BARDEX II took place over a 3-month period from May to July 2012 in the Delta Flume, the Netherlands, and involved over 30 staff from 8 different institutions and an ambitious test program. The project was structured into 6 work packages, each led by a different institution and representing a different phase of the test program and/or a different region on the barrier profile. Such clear organizational framework considerably simplified the logistics with respect to planning the attendance of participants and made it possible to complete all planned tests within the allocated time.

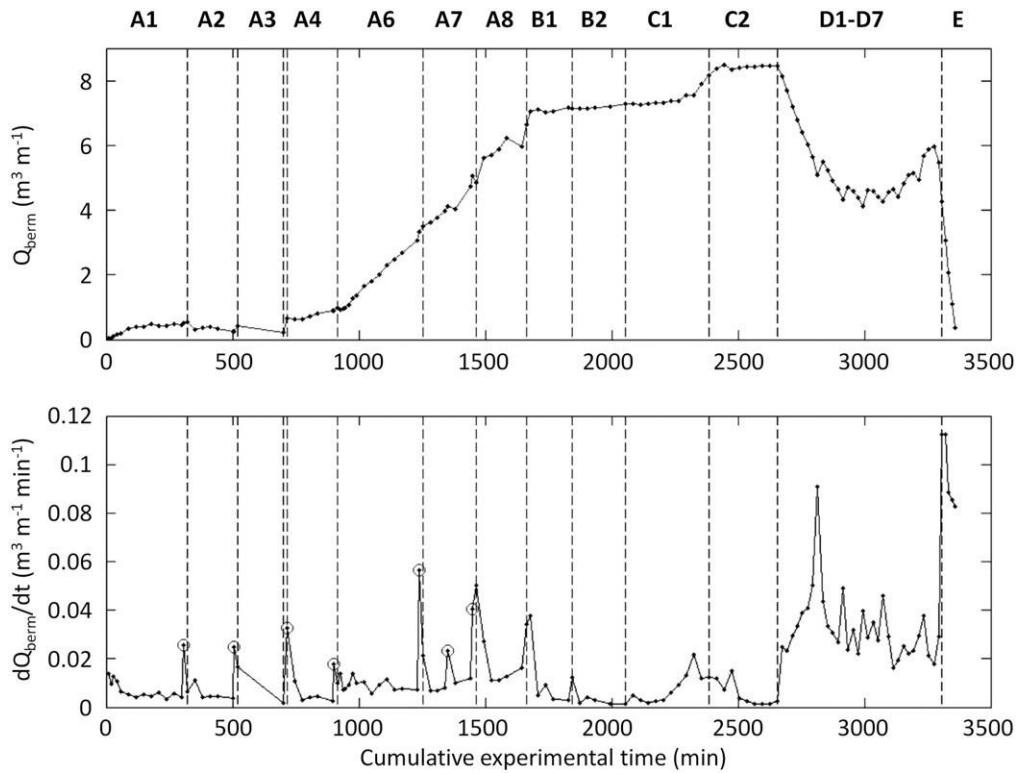


Fig. 12. Change in sediment volume of the upper beach ('berm') region of the beach ($x = 90\text{--}110\text{ m}$) Q_{berm} relative to the start of the experiment and the gross rate of volumetric change over this region dQ_{berm}/dt for each test, over the experimental period. Circles in the lower panel represent tests with mono-chromatic waves. Test A5, which involved 8 short sequences of mono- and bi-chromatic wave action (2 min each), was conducted between tests A3 and A4.

Tests during BARDEX II were designed to ensure sufficient morphological change would occur during the tests to determine morphological trends, not to determine the equilibrium morphology. For practical reasons, the beach profile was not reshaped between different tests, such that the morphology developed cumulatively and each test started with a different morphological boundary condition. In that sense, the tests were rather different from the Large Wave Tank experiments carried out, e.g., in 1956–1957 and 1962 by the US Army Corps of Engineers (Kraus and Larson, 1988), with each test condition generally lasting more than 50 hours and each test starting with the same initial morphology. The BARDEX II tests are also quite different from those during the first BARDEX when the tests were of similar duration, but Preparations for the experiment, which included computer simulations quasi-equilibrium developed after only several hours of wave action to inform instrument positioning based on the expected morphological response, were made assuming that sediment with a sediment (Masselink and Turner, 2012).

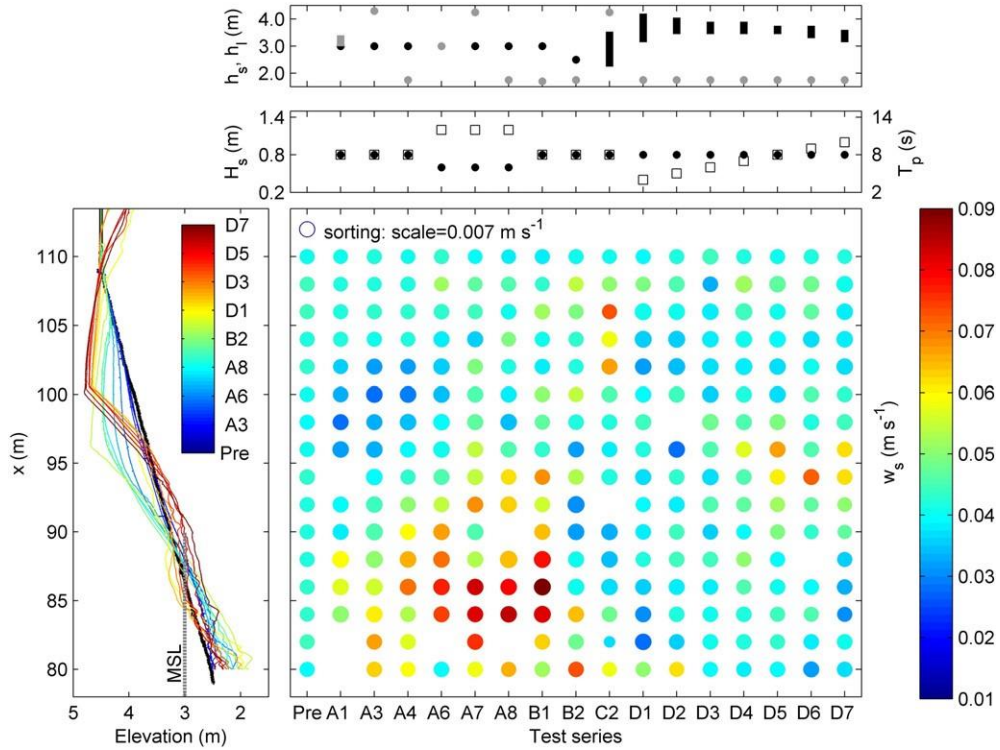


Fig. 13. Time series of sea level h_s (black symbols) and lagoon level h_l (gray symbols), and significant wave height H_s (black circles) and peak wave period T_p (white squares) during the experiment (top two panels); beach profiles after each of test (left panel); and spatial and temporal variability in the sediment fall velocity (color of the symbol) and sorting (size of the symbol).

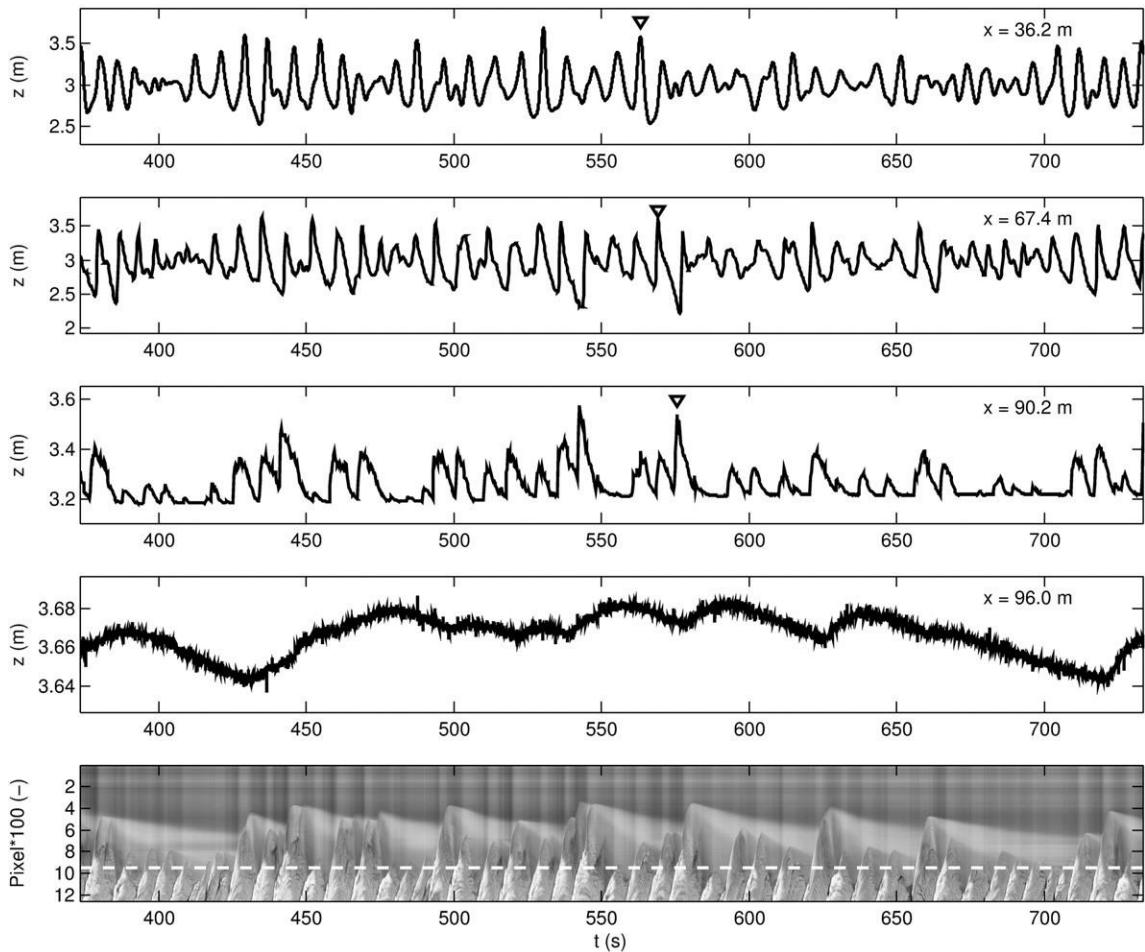


Fig. 14. Example of 6 min of data collected during run no. 2 of test A2 (A2_02) showing landward transformation of the wave signal. From top to bottom: shoaling waves at $x = 36.2$ m measured with Delta Flume PT; breaking waves at $x = 67.4$ m measured with UU PT; swash action at $x = 90.2$ m measured with UNSW BLS; beach groundwater table at $x = 96.0$ m measured with Delta Flume PT; and timestack showing swash action measured with Delta Flume video camera. The down-facing triangle marks the propagation of a wave through the instrument array, up to the top of the beach. The dashed horizontal line in the bottom panel indicates the position of the BLS sensor used in the third panel.

size D_{50} of 0.6–0.8 mm and a sediment fall velocity w_s of 0.8 m s^{-1} could be obtained. However, 2 months before the start of the project, it became known that the requested sediment was not available and the barrier was constructed out of significantly finer sediment ($D_{50} = 0.43 \text{ mm}$; $w_s = 0.46 \text{ m s}^{-1}$). There was insufficient time to modify the test program to reflect the different sediment size, and the erosive beach response during the first part of the experiment (tests A1–A4) was not anticipated, requiring ad hoc changes to be made to the test program. Unplanned changes to the experimental design, such as the provision of a smaller sediment size, can have important consequences and so should be made with as much notice as possible.

The production of the final report and the collation of the complete data set for future use for a project of the scale of BARDEX II is a very significant task. Ideally, a dedicated person should be appointed to participate in the experiment, responsible for diarizing the experiment and ensuring the documentation is complete, as well as producing the final report and data set. For BARDEX II, these tasks were carried out by the PI and a post-doc appointed after the experiment. The latter spent c. 6 months of their time collating and error-checking the NetCDF data set. The provision of a self-explanatory data-set from a large experiment is a time-consuming task that is rarely undertaken, but which will be increasingly expected due to pressures from funding bodies to make data open-access.

The preliminary findings of BARDEX II were published in a special issue of *Journal of Coastal Research* and the key findings are reported in this special issue, with additional research outputs published in other outlets (e.g., Dubarbier et al., 2015; Kassem et al., submitted for publication) and in preparation. Many of the new research findings are related to fundamental nearshore hydro- and morphodynamics with the novel understanding gained through the controlled nature of the forcing conditions and the extensive and advanced instrumentation used. Turner et al. (2016) observed that the groundwater level, flow paths, and fluxes within the beach face region of the barrier were predominantly controlled by the action of waves at the beach face, regardless of the overall seaward- or landward-directed barrier-scale hydraulic gradients. According to Blenkinsopp et al. (2016), both extreme runup and the lower limit of the swash zone, which was consistently below the SWL, scaled well with the deep water Iribarren number. The vertical runup excursion of each swash was also correlated strongly with the height of the bore at collapse and could be predicted based on the assumption of a conversion of potential to kinetic energy at bore collapse. Measurements of overwash dynamics by Matias et al. (2016) revealed that overwash volumes are strongly and positively related to the incident wave period and that there is limited potential for crestral build-up when the barrier is being overtopped. Ruessink et al. (2016) found that sand bar formation under erosive waves occurred with minimal sediment exchange between swash and surf zone and that berm dynamics under accretionary waves were governed primarily by wave conditions and antecedent morphology. Brinkkemper et al. (2016) demonstrated that the vertical turbulence structure in the surf zone evolved from bottom-dominated (bed shear stress) to surface-dominated (bore-generated) with an increase in the fraction of breaking waves to ~50%. In the swash zone, the turbulence was predominantly bottom-induced during the backwash and showed a homogeneous turbulence profile during uprush. Using the data collected under mono-chromatic wave conditions, Puleo et al. (2016) found that the instantaneous sediment flux magnitudes in the sheet flow layer were nearly always larger than those for suspended sediment flux; however, sediment transport rates integrated over depth indicated that suspended load transport was generally dominant during uprush and during the early stages of backwash. Ruju et al. (2016) demonstrated that the cross-shore velocity profiles measured in the swash zone were well represented by the logarithmic model. Friction factors estimated from the logarithmic profile were of the same order of magnitude for the uprush and the backwash, but with a strong variability related to the boundary layer growth during the backwash.

Some of the new research findings reported in the papers in this BARDEX II special issue can be compared with, and add value to, the BARDEX gravel barrier experiment (Williams et al., 2012a). The most noticeable difference between the two experiments is related to the morphological response. Beach change on the gravel barrier was significantly faster with a quasi-steady equilibrium established within several hours of wave action (Masselink and Turner, 2012), whereas equilibrium was never attained on the sandy barrier. Additionally, onshore sediment transport and berm construction was dominant on the gravel barrier (Masselink and Turner, 2012), whereas onshore as well as offshore sediment transport and berm as well as bar development occurred on the sandy barrier (Ruessink et al., 2016). Matias et al. (2016) compared the morphologic response to overwash on both barriers, and during both experiments, the sea level was progressively raised to study the transition from swash to overtopping to overwash. The comparative analysis showed that on the gravel barrier crestral build-up during the overtopping stage delayed the occurrence of overwash, whereas on the sandy barrier, nearshore bar development played a similar role. In both cases, the morphological development represented a negative morphodynamic feedback, improving the stability of the barrier system. The effect of the different sediment size and hydraulic conductivity, and therefore on the groundwater dynamics, between the two sets of experiments was also noted. A comparison in the over-height of the water table in the swash zone due to the presence of waves revealed a significantly larger over-height in the sandy barrier (Turner and Masselink, 2012; Turner et al., 2013). Moreover, whereas for the gravel barrier, the over-height was independent of the lagoon level, this was not the case for sandy barrier (Turner et al., 2016). Manipulating the beach groundwater table by changing the lagoon level had a very significant impact on the beach profile development on the gravel barrier, with a low lagoon level encouraging beach accretion in the swash zone and a high lagoon level promoting beach erosion (Masselink and Turner, 2012). The groundwater effect on the sandy barrier was less significant and ground water gradients in the beach were only relevant to berm dynamics when the berm was in the early stages of development (Ruessink et al., 2016). The measurements of Ruju et al. (2016) of the vertical velocity profiles in the swash zone of the sandy barrier suggested that, under identical wave forcing but varying lagoon level, bed shear stresses are weaker during the latter stages of the backwash when the lagoon level is high, supposedly due to exfiltration. This seems to confirm and extend the corresponding results observed for gravel barriers (Masselink and Turner, 2012).

To conclude, a very comprehensive, high-quality, and freely available data set has been collected in this large-scale laboratory experiment. It is hoped and expected that the BARDEX II team, as well as other researchers, will use these data to provide fundamental new information and understanding on cross-shore sediment transport processes in the nearshore zone of sandy beaches.

Acknowledgements

The work described in this publication was supported by the European Community's 7th Framework Programme through the grant to the budget of the Integrating Activity HYDRALAB IV, contract no. 261520. Collation of the BARDEX II data set was made possible by the EPSRC grant Proto-type Experiment and Numerical Modelling of Energetic Sediment Transport under Waves (PESTS; EP/K000306/1). A. Matias was supported by RUSH project (From Runup to Overwash), PTDC/CTE-GIX/ 116814/2010 financed by FCT. The academic lead of the project was Gerd Masselink and the Deltares coordinator was Guido Wolters. The BARDEX II partners would like to thank the Delta Flume staff (Leen, Johan, Piet, and Ab) for making the experiment such an enjoyable and successful experience. The full BARDEX data set is available from www.hydralab.info.

References

- Aagaard, T., Hughes, M., Moller-Sorensen, R., Andersen, S., 2006. Hydrodynamics and sediment fluxes across an onshore migrating intertidal bar. *J. Coast. Res.* 22, 247–259.
- Andersen, M.S., Baron, L., Gudbjerg, J., Chapellier, D., Jakobsen, R., Gregersen, J., Postma, D., 2007. Nitrate-rich groundwater discharging into a coastal marine environment. *J. Hydrol.* 336, 98–114.
- Blenkinsopp, C., Matias, A., Howe, D., Castelle, B., Marieu, V., Turner, I.L., 2016. Wave runup and overwash on a prototype-scale sand barrier. *Coast. Eng.* 113, 88–103.
- Brinkkemper, J., Lanckriet, T., Grasso, F., Puleo, J., Ruessink, G., 2016. Observations of turbulence within the surf and swash zone of a field-scale sandy laboratory beach. *Coast. Eng.* 113, 62–72.
- Butt, T., Russell, P.E., Puleo, J., Miles, J., Masselink, G., 2004. Influence of bore turbulence on sediment transport in the swash and inner surf zones. *Cont. Shelf Res.* 24, 757–771.
- Castelle, B., Dubarbier, B., Tissier, M., Bonneton, P., Conley, D.C., Ruessink, B.G., Masselink, G., 2013. Testing numerical hydrodynamic and morphodynamic models against BARDEX II Experiment data sets. *J. Coast. Res.* SI65, 1745–1750.
- Conley, D.C., Inman, D.L., 1992. Field observations of the boundary layer under near breaking waves. *J. Geophys. Res.* 97, C6.
- Conley, D.C., Falchetti, S., Lohmann, I.P., Brocchini, M., 2008. The effects of flow stratification by non-cohesive sediment on transport in high-energy wave-driven flows. *J. Fluid Mech.* 610, 43–67.
- Dubarbier, B., Castelle, B., Marieu, V., Ruessink, B.G., 2015. On the modeling of sandbar formation over a steep beach profile during the large-scale wave flume experiment Bardex II. *Proceedings Coastal Sediments 2015*. ASCE, San Diego.
- Falchetti, S., Conley, D.C., Brocchini, M., Elgar, S., 2010. Nearshore bar migration and sediment-induced buoyancy effects. *Cont. Shelf Res.* 30, 226–238.
- Foster, D.L., Bowen, A.J., Holman, R.A., Natoo, P., 2006. Field evidence of pressure gradient induced incipient motion. *J. Geophys. Res.* 111, C05004.
- Hoefel, F., Elgar, S., 2003. Wave-induced sediment transport and bar migration. *Science* 299, 1885–1887.
- Kassem, H., Thompson, C.E.L., Amos, C.L., Townend, I.H., 2015. Wave-induced coherent turbulence structures and sediment resuspension in the nearshore of a prototypical sandy barrier beach, Barrier Dynamics Experiment II. *Cont. Shelf Res.* (submitted for publication).
- Kraus, N.C., Larson, M., 1988. Beach Profile Change Measured in the Tank for Large Waves, 1956-1957 and 1962. Tech. Rep. CERC-88-6. U.S. Army Engineers Waterways Experiment Station, Vicksburg, MS.
- Lanckriet, L., Puleo, J.A., Masselink, G., Turner, I.L., Conley, D., Blenkinsopp, C., Russell, P., 2013. A comprehensive field study of swash zone processes, Part 2: Sheet flow sediment concentrations during quasi-steady backwash. *J. Waterw. Port Coast. Ocean Eng.* [http://dx.doi.org/10.1061/\(ASCE\)WW.1943-5460.0000209](http://dx.doi.org/10.1061/(ASCE)WW.1943-5460.0000209).
- Lopez de San Roman-Blanco, B., Coates, T.T., Holmes, P., Chadwick, A.J., Bradbury, A., Baldock, T.E., Pedrozo-Acuna, A., Lawrence, J., Grune, J., 2006. Large scale experiments on gravel and mixed beaches: experimental procedure, data documentation and initial results. *Coast. Eng.* 53, 349–362.
- Marino-Tapia, I., Russell, P.E., O'Hare, T., Davidson, M.A., Huntley, D.A., 2007. Cross-shore sediment transport on natural beaches and its relation to sandbar migration patterns Part I: Field observations and derivation of a transport parameterization. *J. Geophys. Res.* 112, C03001.
- Masselink, G., Turner, I.L., 2012. Large-scale laboratory investigation into the effect of varying back-barrier lagoon water levels on gravel beach morphology and swash zone sediment transport. *Coast. Eng.* 63, 23–38.
- Matias, A., Ferreira, O., Vila-Concejo, A., Garcia, T., Dias, J.A., 2008. Classification of washover dynamics in barrier islands. *Geomorphology* 97, 655–674.
- Matias, A., Williams, J., Ferreira, O., Masselink, G., 2012. Overwash threshold for gravel barriers. *Coast. Eng.* 63, 48–61.
- Matias, A., Masselink, G., Kroon, A., Blenkinsopp, C., Turner, I.L., 2013. Overwash experiment on a sandy barrier. *J. Coast. Res.* SI 65, 778–783.
- Matias, A., Masselink, G., Castelle, B., Blenkinsopp, C., Kroon, A., 2016. Measurements of morphodynamic and hydrodynamic overwash processes in a large-scale wave flume. *Coast. Eng.* 113, 33–46.
- Puleo, J.A., Blenkinsopp, C., Conley, D., Masselink, G., Turner, I.L., Russell, P., Buscombe, D., Howe, D., Lanckriet, T., McCall, R., Poate, T., 2013. A comprehensive field study of swash-zone hydrodynamics, Part 1: Experimental design with examples of hydrodynamic and sediment transport processes. *J. Waterw. Port Coast. Ocean Eng.* [http://dx.doi.org/10.1061/\(ASCE\)WW.1943-5460](http://dx.doi.org/10.1061/(ASCE)WW.1943-5460).
- Puleo, J., Lanckriet, T., Conley, D., Foster, D., 2016. Sediment transport partitioning in the swash zone of a large scale laboratory beach. *Coast. Eng.* 113, 73–87.
- Ruessink, B.G., Blenkinsopp, C., Brinkkemper, J.A., Castelle, B., Dubarbier, B., Grasso, F., Puleo, J., Lanckriet, T., 2016. Sandbar and beach-face evolution on a prototype coarse sandy barrier. *Coast. Eng.* 113, 19–32.
- Ruju, A., Conley, D.C., Masselink, G., Austin, M., Puleo, J., Lanckriet, T., Foster, D., 2016. Boundary layer dynamics in the swash zone under large-scale laboratory conditions. *Coast. Eng.* 113, 47–61.
- Ruju, A., Conley, D., Masselink, G., Austin, M., Puleo, J., 2015. Sediment transport dynamics in the swash zone under large-scale laboratory conditions. *Cont. Shelf Res.* (submitted for publication).
- Sanchez-Arcilla, A., Caceres, I., van Rijn, L., Grune, J., 2011. Revisiting mobile bed tests for beach profile dynamics. *Coast. Eng.* 58, 583–593.
- Stratigakia, V., Manca, E., Prinos, P., Losada, I.J., Lara, J.L., Scavo, M., Amos, C.L., Caceres, I., Sanchez-Arcilla, A., 2011. Large-scale experiments on wave propagation over *Posidonia oceanica*. *J. Hydraul. Res.* 49, 31–43.
- Thompson, C.E.L., Williams, J.J., Metje, N., Coates, L.E., Pacheco, A., 2012. Turbulence based measurements of wave friction factors under irregular waves on a gravel bed. *Coast. Eng.* 63, 39–47.
- Thompson, C.E.L., Kassem, H., Williams, J., 2013. BARDEX II: nearshore sediment resuspension and bed morphology. *J. Coast. Res.* SI 65, 1593–1598.
- Turner, I.L., Masselink, G., 1998. Swash infiltration-exfiltration and sediment transport. *J. Geophys. Res.* 103, 30,813–30,824.
- Turner, I.L., Masselink, G., 2012. Barrier coastal gravel barrier hydrology – observations from a prototype-scale laboratory experiment (BARDEX). *Coast. Eng.* 63, 13–22.
- Turner, I.L., Russell, P.E., Butt, T., 2008. A new instrumentation to measure wave-by-wave bed-levels in the swash zone. *Coast. Eng.* 55, 1237–1242.
- Turner, I.L., Rau, G.C., Andersen, M.S., Austin, M.J., Puleo, J., Masselink, G., 2013. Coastal sand barrier hydrology – observations from the BARDEX II prototype-scale laboratory experiment. *J. Coast. Res.* SI 65, 1886–1891.
- Turner, I.L., Rau, G.C., Austin, M.J., Andersen, M.S., 2016. Groundwater fluxes and flow paths within coastal barriers: observations from a large-scale laboratory experiment (BARDEX II). *Coast. Eng.* 113, 104–116.
- Williams, J., Buscombe, D., Masselink, G., Turner, I.L., Swinkels, C., 2012a. Barrier Dynamics Experiment (BARDEX): aims, design and procedures. *Coast. Eng.* 63, 3–12.
- Williams, J.J., Ruiz de Alegria-Arzaburu, A., McCall, R.T., van Dongeren, A., 2012b. Modelling gravel barrier profile response to combined waves and tides using XBeach: laboratory and field results. *Coast. Eng.* 63, 62–80.
- Winter, W. de, D., Wesselman, Grasso, F., Ruessink, G., 2013. Large-scale laboratory observations of beach morphodynamics and turbulence beneath shoaling waves and plunging breakers. *J. Coast. Res.* SI65, 1515–1520.